



OPEN ACCESS

EDITED BY

Riccardo Dolcetti,
Peter MacCallum Cancer Centre, Australia

REVIEWED BY

Shuzhao Chen,
First Affiliated Hospital of Shantou University
Medical College, China
Annarita Nappi,
University of Naples Federico II, Italy

*CORRESPONDENCE

Yuchao Gu
[✉ guych@126.com](mailto:guych@126.com)
Xiao Wu
[✉ wuxiao457891@outlook.com](mailto:wuxiao457891@outlook.com)
Changning Sun
[✉ scn199574@outlook.com](mailto:scn199574@outlook.com)

[†]These authors have contributed equally to this work

RECEIVED 18 February 2025

ACCEPTED 19 May 2025

PUBLISHED 30 May 2025

CITATION

Wang Z, Sun C, Wang P, Lin S, Wu X and Gu Y (2025) Pan-cancer analysis of TMED2: unraveling potential immune characteristics and prognostic value in cancer therapy. *Front. Immunol.* 16:1578627.
doi: 10.3389/fimmu.2025.1578627

COPYRIGHT

© 2025 Wang, Sun, Wang, Lin, Wu and Gu. This is an open-access article distributed under the terms of the [Creative Commons Attribution License \(CC BY\)](#). The use, distribution or reproduction in other forums is permitted, provided the original author(s) and the copyright owner(s) are credited and that the original publication in this journal is cited, in accordance with accepted academic practice. No use, distribution or reproduction is permitted which does not comply with these terms.

Pan-cancer analysis of TMED2: unraveling potential immune characteristics and prognostic value in cancer therapy

Zhuangzhi Wang^{1,2†}, Changning Sun^{1*†}, Pengfei Wang³,
Shouyang Lin^{1,2}, Xiao Wu^{3*} and Yuchao Gu^{1*}

¹Qingdao Center of Technology Innovation for Shark Antibody Development, College of Biological Engineering, Qingdao University of Science and Technology, Qingdao, China, ²School of Medicine and Pharmacy, Ocean University of China, Qingdao, China, ³Department of Respiratory and Critical Care Medicine, Qingdao Central Hospital, University of Health and Rehabilitation Sciences, Qingdao, China

Background: Transmembrane emp24 domain-containing protein 2 (TMED2) is involved in the sorting and transport of proteins between the Golgi apparatus and the endoplasmic reticulum. Recent research has identified a close association between TMED2 and tumorigenesis, yet its regulatory role and underlying mechanisms in pan-cancer signaling pathways remain unexplored.

Methods: We conducted a comprehensive pan-cancer analysis of TMED2 using multiple public databases. These analyses included assessments of prognostic significance, gene mutations, pathway enrichment, single-cell sequencing analysis, immune characteristics, co-expressed gene PPI network analysis, as well as the therapeutic response of TMED2 in immunotherapy and small molecule sensitivity. Finally, we examined the role that TMED2 plays at the cellular level.

Results: Our results show that the mRNA levels of TMED2 differ significantly between cancerous and normal tissues and are closely associated with cancer prognosis. Specifically, in CESC, MESO, LGG, and UVM, overexpression of TMED2 correlates with patient prognosis and various clinical pathological features. TMED2 is significantly associated with immune infiltration (including endothelial cells, neutrophils, dendritic cells, and eosinophils), immune checkpoints (CD274, HAVCR2, PDCD1LG2, and SIGLEC15), and signaling pathways (cell cycle and PI3K/Akt). Single-cell sequencing reveals that TMED2 is predominantly expressed in tumor cells of cervical cancer, glioma, and mesothelioma. Enrichment analysis shows that genes co-expressed with TMED2 are primarily involved in processes like endoplasmic reticulum stress and the ERAD pathway. Furthermore, cellular studies indicated that TMED2 expression promotes the growth, migration and invasion of glioma cells.

Conclusion: Our integrated analysis suggests that targeting TMED2, along with its associated genes and signaling pathways, could represent a new strategy for cancer immune treatment.

KEYWORDS

pan-cancer analysis, immunotherapy, tumor microenvironment, protein transport, TMEDs

1 Introduction

Cancer, as one of the key challenges in global public health, has been a central focus of medical research. With the advancing understanding of cancer pathogenesis, immunotherapy has emerged as a crucial strategy for cancer treatment (1–4). By activating the immune system to identify and destroy cancerous cells, immunotherapy offers new hope for cancer patients. However, the high heterogeneity of cancer results in significant variations in the efficacy of immunotherapy across different cancer types (5, 6). This emphasizes how vital it is to find new biomarkers to better predict patient responses to immunotherapy and optimize treatment strategies.

Transmembrane emp24 domain-containing protein 2 (TMED2) has gained increasing attention in recent years as a key molecule potentially involved in the process of tumorigenesis and development and progression (7, 8). TMED2 is the only member of the β-subfamily within the mammalian TMED family (9). All TMED family members share a similar domain architecture, including an N-terminal Golgi dynamics (GOLD) domain and coil-coiled (CC) domain, a transmembrane domain, and a C-terminal cytoplasmic domain (9). The intracellular physiological functions of TMED2 are complex, and one of its primary functions is mediating protein transportation from the endoplasmic reticulum (ER) to the Golgi apparatus (10). TMED2 binds to proteins destined for transport, facilitates their proper folding and packaging, and delivers them to the Golgi for further modification and processing (11, 12).

As part of the vesicle trafficking system, TMED2 regulates the formation, transport, and fusion of vesicles (13). By interacting with vesicle-associated proteins, it influences the dynamic properties of vesicles, ensuring efficient and accurate intracellular material transport. This regulation is vital for maintaining intracellular homeostasis and normal organelle functions (14). Previous research have revealed aberrant expression of TMED2 in specific cancer types (15). In ovarian cancer, high TMED2 expression has been connected with increased proliferation and invasion of cancer cells (16). Additionally, TMED2 expression has been linked to the development of cancerous cells in breast cancer (17) and head and neck squamous cell carcinoma (18). In the context of cancer, TMED2 may impact tumor growth, metastasis, and its interactions with the immune system. Studies have already analyzed its expression across various human cancer subtypes (8, 19). However, more comprehensive analyses are still lacking, such as protein interaction networks co-expressed with TMED2, single-cell sequencing analyses, and a detailed understanding of its mechanisms in tumor-immune interactions. Therefore, the potential roles and clinical applications of TMED2 in cancer remain to be explored further.

In this study, the prognostic and immune-related functions of TMED2 across pan-cancer were comprehensively examined by using public databases, including TCGA (The Cancer Genome Atlas), GTEx (Genotype-Tissue Expression Program), and CCLE (Cancer Cell Line Encyclopedia). We performed GSEA (Gene Set Enrichment Analysis) pathway enrichment analyses and explored

the correlations between TMED2 levels and genetic mutation statuses in these cancers. Furthermore, TMED2's co-expression in different cell types within the tumor microenvironment was validated through online datasets and single-cell sequencing analysis. We then performed Spearman correlation analysis to identify genes co-expressed with TMED2, followed by protein-protein interaction (PPI) network analysis and enrichment analyses using Gene Ontology (GO) and Kyoto Encyclopedia of Genes and Genomes (KEGG) pathways. We also predicted potential immunotherapy efficacy and drug sensitivity targeting TMED2 in these cancers. Finally, experimental validation was conducted to evaluate the impact of TMED2 knockdown on abnormal biological behaviors, such as proliferation, in glioma cells. In summary, TMED2 has promise as an effective target and a biomarker for predicting treatment responses in cancer therapy.

2 Materials and methods

2.1 Open data collection

TCGA RNA-seq data and metadata were obtained from the UCSC Xena platform (<https://xenabrowser.net/>). The scRNA-seq data including cervical cancer (GSE168652), glioma (GSE131928) and mesothelioma (GSE201925) was downloaded from GEO (<https://www.ncbi.nlm.nih.gov/geo/>). The drug-susceptibility and cell line DATA was downloaded from GDSC (<https://www.cancerrxgene.org/>), CCLE (<https://sites.broadinstitute.org/cdle/>) and CellMiner (https://discover.nci.nih.gov/cell_miner/home.do).

2.2 Single-cell sequencing analysis

The R package (Seurat v5.2) were applied for scRNA-seq data integration and quality control (13). Cells were filtered based on the following criteria: nFeature_RNA > 200, percent.mt < 20, nCount_RNA > 800, and percent.hb < 5. Dimensionality reduction using Principal Component Analysis (PCA). The Harmony package was used for data integration. The FindClusters function was applied to cluster the cells together. Visualization of dimensionality reduction with UMAP functions. Marker genes utilized for the annotation of cell clusters were presented in Supplementary Table S3.

2.3 Research on the prognostic and immune roles of TMED2

The overall survival (OS) and progression free interval (PFI) were analyzed using the Kaplan-Meier (KM) curve. The IOBR package was used to assess the immunological landscapes of TMED2 (20). The reactions of TMED2 to immunotherapy and gene treatment in these tumors were examined using the TIDE (<http://tide.dfci.harvard.edu>) and ROC plotter (<https://rocplot.org/>)

resources. The MuTarget (<https://www.mutarget.com/analysis?type=target>) was used to examine the association between TMED2 expression and various mutations in gene status within these malignancies. Using the clusterProfiler package, the Gene Set Enrichment Analysis (GSEA), Kyoto Encyclopedia of Genes and Genomes pathway analysis (KEGG) and Gene Ontology enrichment analysis (GO) was used to find rich signaling pathways (21). The scRNA-seq analysis was followed by the pipeline of Seurat (v5.2). The PPI-network was construct by the STRING (<https://cn.string-db.org/>) and the corresponding results were utilized by the STRINGdb package.

2.4 Cell culture

The cell lines HEK293T, U87 and U251 were obtained from the Stem Cell Bank, Chinese Academy of Sciences. And the cells were cultivated in DMEM (Gibco, #11965092) medium with 10% FBS (PAN Biotech, #ST30-3302).

2.5 Generation of cell lines

PEI (Sigma-Aldrich, #764604) was used as the transfection reagent, and pMD2.G (Addgene, #12259), psPAX2 (Addgene, #12260) and pLKO.1 shRNA vector were co-transfected into HEK293T cells. After transfection, cell supernatants were collected at 48 h and 72 h, respectively, and filtered using a 0.45 μ m filter to remove cellular debris to obtain a viral suspension. Subsequently, the viral suspension was used to infect the target cells for 48 hours. To screen successfully infected cells, puromycin (2 μ g/mL, MCE, #HY-K1057) was conducted to resistance screening for one to two weeks to obtain stable pLKO.1 shRNA expressing cell lines. TMED2 shRNA targeting sequence: GGACATCGACGTGGAGATTAC.

2.6 Western blotting

Cells were lysed in RIPA buffer (Epizyme Biotech, #PC101) with complete protease inhibitors (TargetMol, #C0001) and phosphatase inhibitors (Beyotime Biotechnology, #P1081 and P1086). Then cell debris was removed by centrifugation. Protein samples were separated by SDS-PAGE and transferred onto Immobilon-FL PVDF membrane (0.45 μ m, Merck Millipore, #IPVH00005). After transfer, the membranes were blocked with 4% BSA for 1 h, followed by incubation with the indicated antibodies at 4°C overnight. The following day, the membranes were washed three times with TBST for 10 minutes each time and then incubated with the corresponding secondary antibody for 1 hour at room temperature. Finally, the target protein bands were developed using ECL chromogenic solution (Shandong Sparkjade Biotechnology Co., Ltd., #ED0015). Image J software was used to quantitatively evaluate the bands, using either β -actin or GAPDH to be the internal reference control. The antibodies used in the experiment are shown in [Supplementary Table S1](#).

2.7 RT-qPCR

Total RNA was extracted using QIAGEN RNeasy Mini Kit (Qiagen, #74104) for RT-qPCR experiments. Subsequently, RNA was reverse transcribed into cDNA using HiScript III 1st Strand cDNA Synthesis Kit (Vazyme Biotech Co., Ltd., #R312). Mixing cDNA template obtained from reverse transcription with specific primers and SYBR Green qPCR mix (Shandong Sparkjade Biotechnology Co., Ltd., #AH0104) to construct the reaction system. The reaction system was constructed. The reaction was performed on an ABI-7500 Real-time PCR system. The relative expression levels of the target genes were evaluated by the $2^{-\Delta\Delta Ct}$ method, and β -actin was used as the internal reference gene for normalization. The primers were synthesized by RuiboBio (Qingdao, China) displayed in [Supplementary Table S2](#).

2.8 Tumor phenotype analysis

Cell viability assay: Cells were treated and inoculated in 96-well plates, each well was filled with CCK-8 solution (Yeasen, #40203ES76), which was then incubated for 1.5 hours at 37°C. Cell viability was evaluated by measuring absorbance at 450 nm.

Colony formation assay: 500 cells per well were inoculated in six-well plates for about 10–15 days. The colonies underwent fixation using 4% paraformaldehyde (PFA). Subsequently, the colonies were subjected to staining with 0.1% crystal violet and photographed.

Cell migration assay: 3×10^4 cells were digested with trypsin, suspended in serum-free medium, and added to the upper chamber of Transwell (pore size 8 μ m, Corning). The lower chamber was filled with a medium that included serum. After removal of nonmigrating cells, they were fixed with 4% PFA, colored with 0.1% crystalline violet, and photographed for evaluation.

2.9 Statistical analysis

Data are shown as the mean \pm standard deviation (M \pm SD). Statistical analyses were performed using GraphPad Prism 9, with significance levels defined as * $P < 0.05$, ** $P < 0.01$ and *** $P < 0.001$. R version 4.3.1 was used to make all bioinformatic and statistical analyses. The Wilcoxon rank-sum test was accustomed to estimate levels of TMED2 expression based on pathological features. Log-rank tests were used to calculate the survival probability using Kaplan-Meier survival curves. Student's t-test was performed using parametric tests (unpaired two-tailed Student's t-test) and nonparametric testing (Mann-Whitney test), determined by whether test assumptions were met. The figure legends of every dataset list the precise tests that were employed.

3 Results

3.1 TMED2 expression and prognosis

First, we examined the mRNA expression levels of paired normal and malignant tissues using TCGA database. The findings

demonstrated that TMED2 expression was increased in BLCA, BRCA, COAD, ESCA, HNSC, KIRC, KIRP, LIHC, LUAD, LUSC, PRAD, and STAD compared to their normal tissue counterparts (*Supplementary Figure S1A*). Subsequently, we combined the TCGA and GTEx databases for a more comprehensive analysis of TMED2 mRNA expression in pan-cancer. TMED2 was significantly upregulated in a wide range of cancers, including ACC, BLCA, BRCA, CESC, CHOL, COAD, DLBC, ESCA, GBM, HNSC, KICH, KIRC, KIRP, LGG, LIHC, LUAD, LUSC, OV, PAAD, PRAD, READ, SARC, SKCM, STAD, TGCT, THYM, UCEC, and UCS, while only LAML exhibited downregulated TMED2 expression (*Figure 1A*). Additionally, we analyzed the expression of TMED2 across different cancer stages and tumor histology. The results showed that in the clinical staging of CESC and pathological tumor staging of MESO, the expression of TMED2 was higher in stages I and IV compared to stages II and III (*Supplementary Figures S1B, C*). In the histological grading of LGG, TMED2 expression was higher in grade G3 than in grade G2 (*Supplementary Figure S1D*). Among histological classifications, TMED2 expression was highest in the adenosquamous carcinoma of CESC and the epithelioid subtype of UVM (*Supplementary Figures S1E, F*). These results showed that TMED2 might be involved in the development and progression of different cancers.

Next, we investigated the prognostic significance of TMED2 across different cancer types. TMED2 was found to act as a risk factor in the progression of many tumors. Univariate Cox regression analysis revealed that increased TMED2 expression was strongly related with poor overall survival (OS) in CESC, KICH, KIRP, LGG, LUAD, MESO, SARC, THCA, and UVM (*Figure 1B*). Additionally, elevated TMED2 expression predicted shorter progression-free intervals (PFI) in ACC, CESC, LGG, MESO, and UVM (*Supplementary Figure S3A*). Furthermore, In CESC, KICH, KIRP, LGG, MESO, and UVM, increased TMED2 expression was associated with decreased disease-specific survival (DSS) (*Supplementary Figure S3H*). We also conducted OS analysis based on the optimal cutoff for TMED2 expression (*Figures 1C-H; Supplementary Figures S2A-F*) and PFI analysis (*Supplementary Figures S3B-G*). These analyses collectively indicate that high TMED2 expression is a significant adverse prognostic factor for patient survival, particularly in cancers such as CESC, LGG, MESO, and UVM.

3.2 Mutation analysis of TMED2 in pan-cancer

Genetic mutations are a fundamental cause of tumorigenesis. Using the MuTarget database, we examined the association between TMED2 expression and genetic mutations in a range of cancer types. The findings revealed that in COAD, higher TMED2 expression was observed in the mutant groups of ZFYVE26, RERE, MYO10, NYAP1, and SEMA4A compared to their wild-type counterparts (*Figure 2A*). In SKCM, TMED2 expression was higher in the wild-type groups of HELZ, ZNF404, FAM133A, and FAM83G compared to their mutant groups, while the opposite

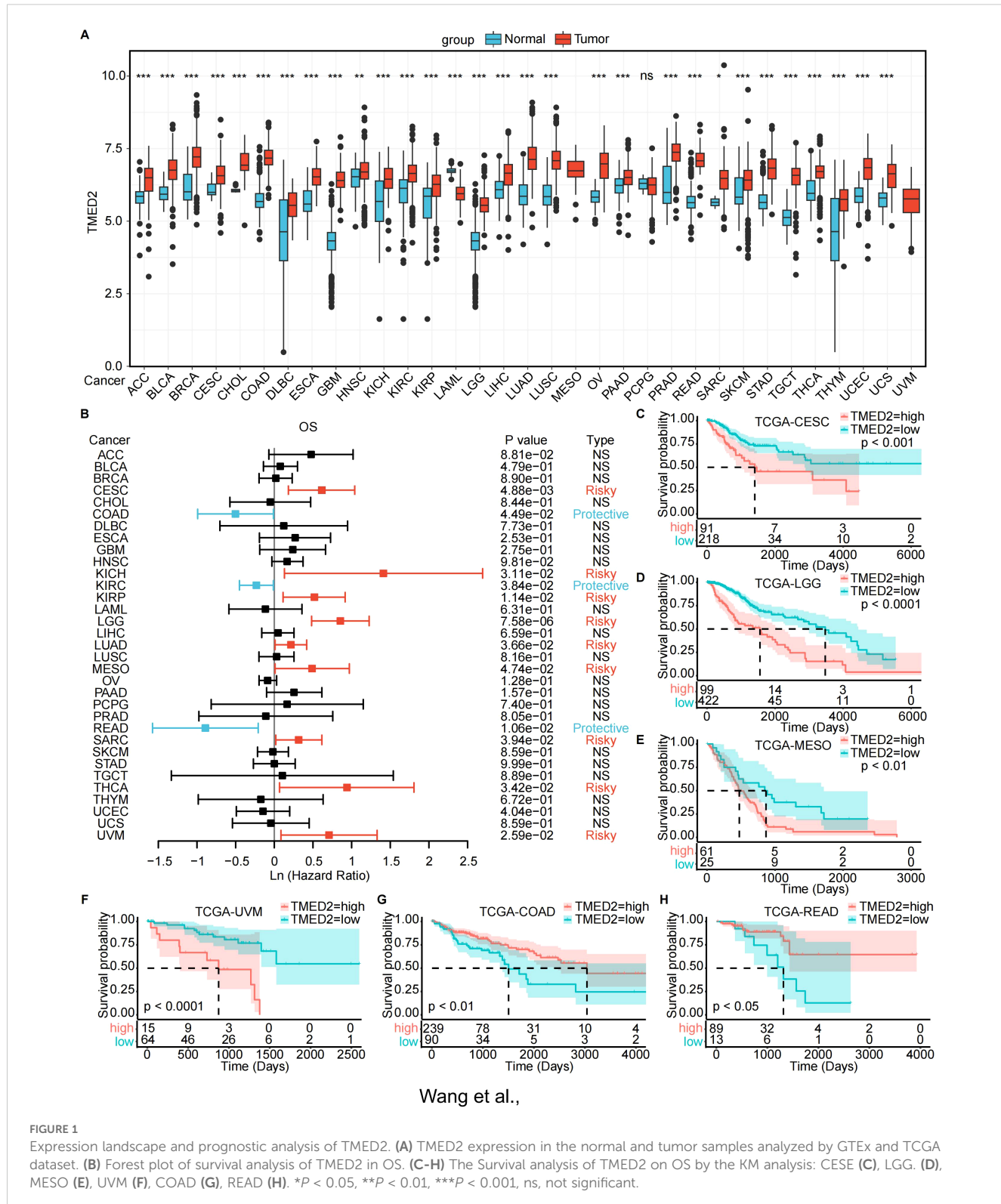
trend was observed for C2CD2 (*Figure 2B*). In STAD, the wild-type groups of multiple genes, including ATP13A2, PPIG, XAB2, LGR6, and ENGASE, exhibited lower TMED2 expression compared to their mutant counterparts (*Figure 2C*). In UCEC, the mutant groups of CCNJ, LRRC3, POU5F2, ODF3L1, and AQP12A showed higher TMED2 expression than the wild-type groups (*Figure 2D*). Additionally, higher TMED2 expression was observed in the mutant groups of TYK2 in BLCA, ARMC9 in CESC, TGM4 and KCNK18 in LUAD, SPON1 and CEP128 in LUSC, and TRDN in SARC compared to their respective wild-type groups. Conversely, the wild-type groups of NBPF10 in CESC, CHD4 in KIRC, SMARCA4 and NFE2L2 in KIRP, OBSCN in SARC, and EPHA7 in OV exhibited higher TMED2 expression than their mutant counterparts (*Supplementary Figure S4*). These mutated genes are involved in critical cellular processes, especially in tumor cells. For instance, SMARCA4 regulates gene expression by remodeling chromatin structure (22), NFE2L2 acts as a key redox transcription factor within cells (23, 24), and LGR6 is a G-protein-coupled receptor 6 that contains leucine-rich repeats (25). These findings highlight the close relationship between TMED2 and genetic mutations in pan-cancer.

3.3 Immunological characteristics of TMED2 in the tumor microenvironment

By stimulating the patient's immune system to identify and combat cancer cells, immunotherapy has become a major focus in cancer treatment research (26–28). We examined several immunological characteristics of TMED2 within the tumor immune microenvironment (TIME) in order to investigate the connection between TMED2 and immunotherapy. Correlations between TMED2 expression levels and stromal, immunological, and ESTIMATE scores were assessed using the ESTIMATE algorithm for a variety of cancer types. DLBC, KIRC, LAML, LGG, THYM, and UCS were the leading six malignancies with a positive connection between TMED2 levels and stromal scores. Among malignancies, the strongest positive correlation between TMED2 levels and immune scores was observed in LGG. The top four cancers with a positive correlation between TMED2 levels and ESTIMATE scores were DLBC, LGG, UCS and UVM (*Figure 3A*).

Subsequently, we applied four immune infiltration algorithms, including CIBERSORT, MCPOUNTER, QUANTISEQ and TIMER, to examine the relationship between TMED2 and immune or stromal cells in various cancers (*Supplementary Figure S5*). The findings showed a positive relationship between TMED2 expression and the infiltration levels of endothelial cells, neutrophils, dendritic cells, and eosinophils in most cancers. In contrast, the expression of TMED2 was negatively correlated with the infiltration levels of monocyte.

We also investigated the relationship between TMED2 and dynamic immune-related features, including two cutting-edge immunotherapy biomarkers: microsatellite instability (MSI) and tumor mutation burden (TMB). TMED2 had a positive correlation with MSI in UCEC, TGCT, STAD, READ, and COAD (*Figure 3B*).

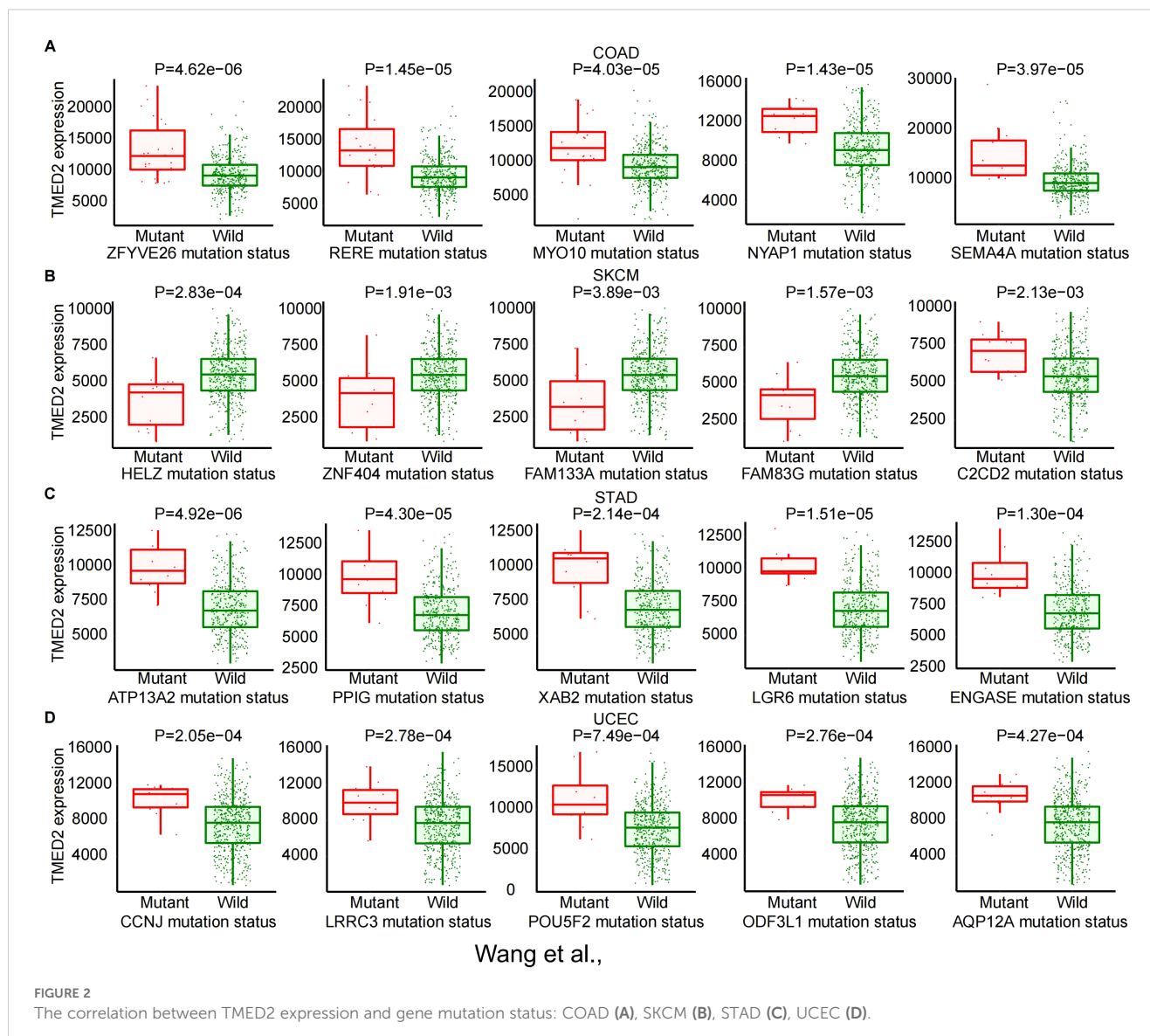


Additionally, TMED2 had a positive correlation with TMB in UCS, THYM, STAD, PAAD, LUAD, LGG, COAD, and BLCA, but a negative correlation with TMB in THCA and CESC (Figure 3C).

Given the notable correlations between TMED2 and immune cells, we examined its relationship with different classical immune checkpoints of cancers. The findings showed a substantial positive

correlation between TMED2 levels and immune checkpoint molecules, including SIGLEC15, PDCD1LG2, HAVCR2, and CD274, in KIRC, LGG, LIHC, OV, PCPG, SKCM, STAD, UCEC and UVM (Figure 3D).

These results imply that TMED2 might play a pivotal role in the tumor immune microenvironment by regulating the characteristics



of immune cells or the expression levels of immunoregulatory genes, thereby influencing cancer growth and response to treatment.

3.4 Functional enrichment analysis of TMED2

To further investigate the potential mechanisms underlying TMED2 function, we performed GSEA analysis in various cancers. In the high TMED2 expression groups of multiple tumor types, pathways related to cell growth and immunity were significantly enriched. Across nearly all cancers, the activation of the PI3K/Akt and cell cycle signaling pathways was positively connected with TMED2 expression (Figure 4A). The PI3K/Akt signaling pathway is essential for a number of physiological processes, such as cell growth, proliferation, differentiation, and

migration. Additionally, TMED2 was significantly associated with NOD-like receptor signaling and antigen processing and presentation pathways in COAD, LGG, LIHC, READ, UCS, and UVM. These findings suggest that TMED2 participates in a number of biological processes and could be crucial to the treatment of cancer.

3.5 Relationship between TMED2 and tumor cells via single-cell sequencing

Next, we examined TMED2 expression in tumor, immune, and stromal cells from a variety of solid tumors types, including cervical cancer, glioma, and mesothelioma (Figures 4B-D). TMED2 demonstrated significant co-expression across tumor cells. Notably, among these cancer types, TMED2 expression was highest in tumor cells, underscoring its potential role in tumor biology.

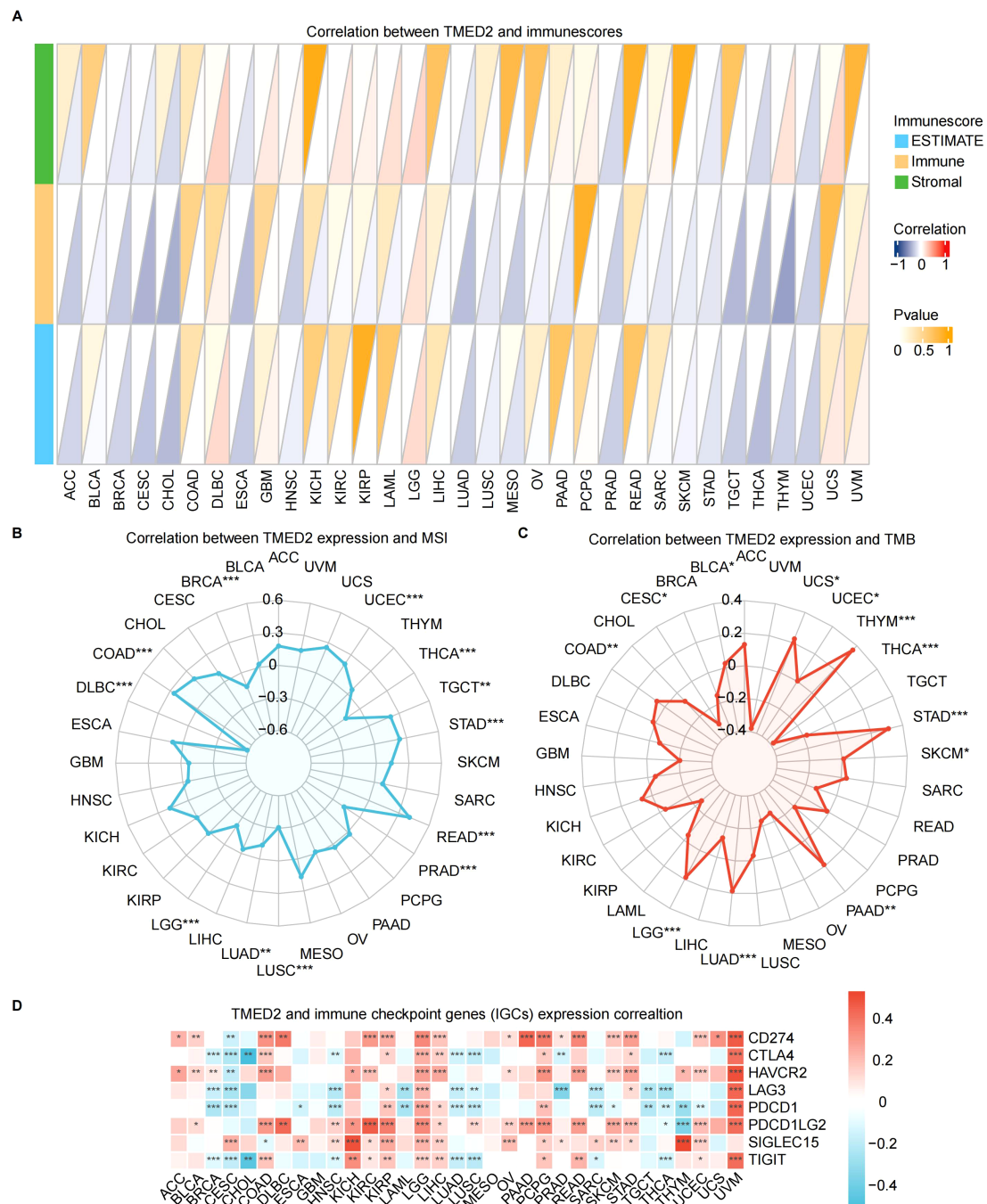


FIGURE 3

FIGURE 3
Relationship of TMED2 expression level with tumor immune characteristics. **(A)** The relationship between TMED2 expression and three scores (immune, estimate, and stromal) in TCGA cancers using ESTIMATE analysis. **(B)** Correlation between TMED2 expression and TMB displayed by the radar chart. **(C)** Correlation between TMED2 expression and MSI displayed by the radar chart. **(D)** Relationship between TMED2 expression and various immune checkpoints. * $P < 0.05$, ** $P < 0.01$, *** $P < 0.001$, ns, not significant.

3.6 Predicting the immunotherapeutic value of TMED2

To systematically explore the potential of TMED2 as an immunotherapy target, we predicted immunotherapeutic responses based on public databases, TIDE scores, a usual and

trustworthy biomarker for predicting immune therapy response, were calculated for patients with different TMED2 expression levels. TMED2 expression and TIDE scores were positively correlated in the majority of solid malignancies, especially in THYM, SARC, LGG, and HNSC (**Figure 5A**). In some solid tumors, non-responders to immunotherapy exhibited higher TMED2

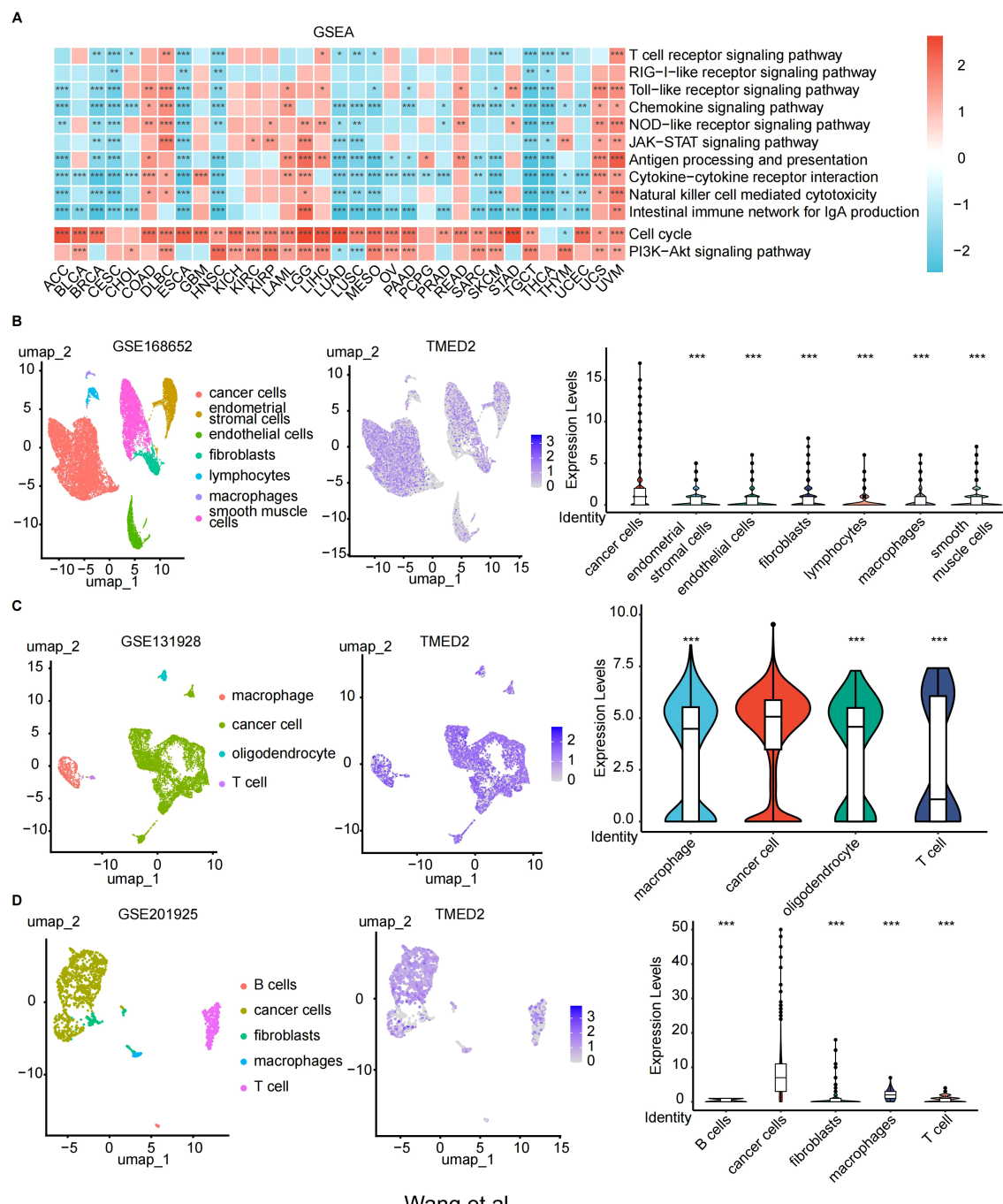


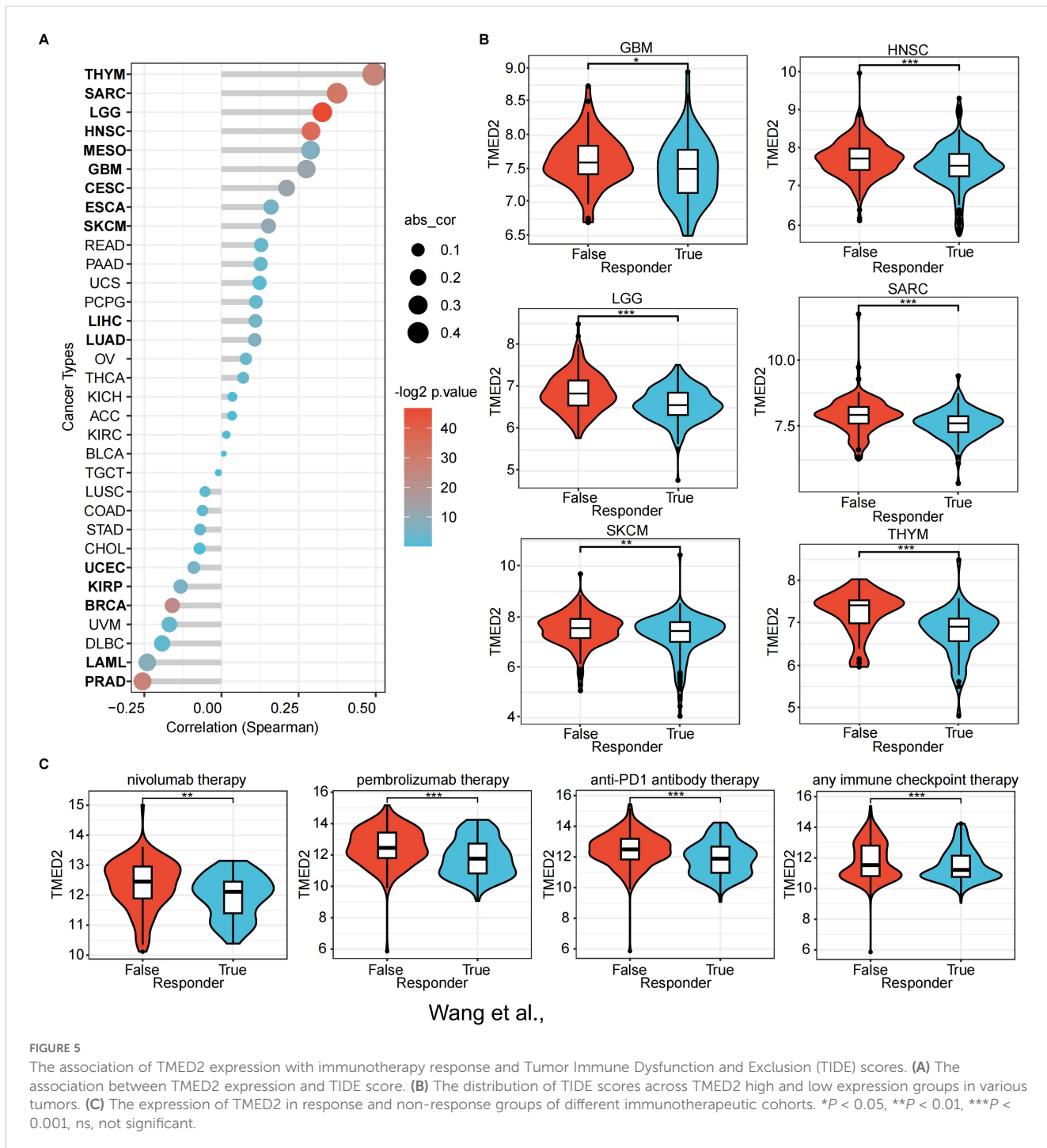
FIGURE 4

FIGURE 4
The relationship of TMED2 expression level with Gene Set Enrichment Analysis (GSEA) and single-cell sequencing. **(A)** Heatmap of the TMED2 pathway enrichment study. **(B-D)** Single-cell sequencing analysis of TMED2 expression in tumor tissues of cervical cancer **(B)**, glioma **(C)**, and MESO **(D)**. * $p < 0.05$, ** $p < 0.01$, *** $p < 0.001$.

expression levels, suggesting reduced therapeutic benefits from immunotherapy (**Figure 5B**).

Using the ROC Plotter dataset, we also analyzed TMED2 expression's predictive value for therapeutic responses in NSCLC, SKCM, HNSC, GBM, and BLCA. The results indicated that higher

TMED2 expression was observed in non-responders to immunotherapies, including nivolumab, pembrolizumab, anti-PD-1, and other immune checkpoint inhibitors (Figure 5C). These findings highlight TMED2 as a potential biomarker for predicting immunotherapy outcomes.

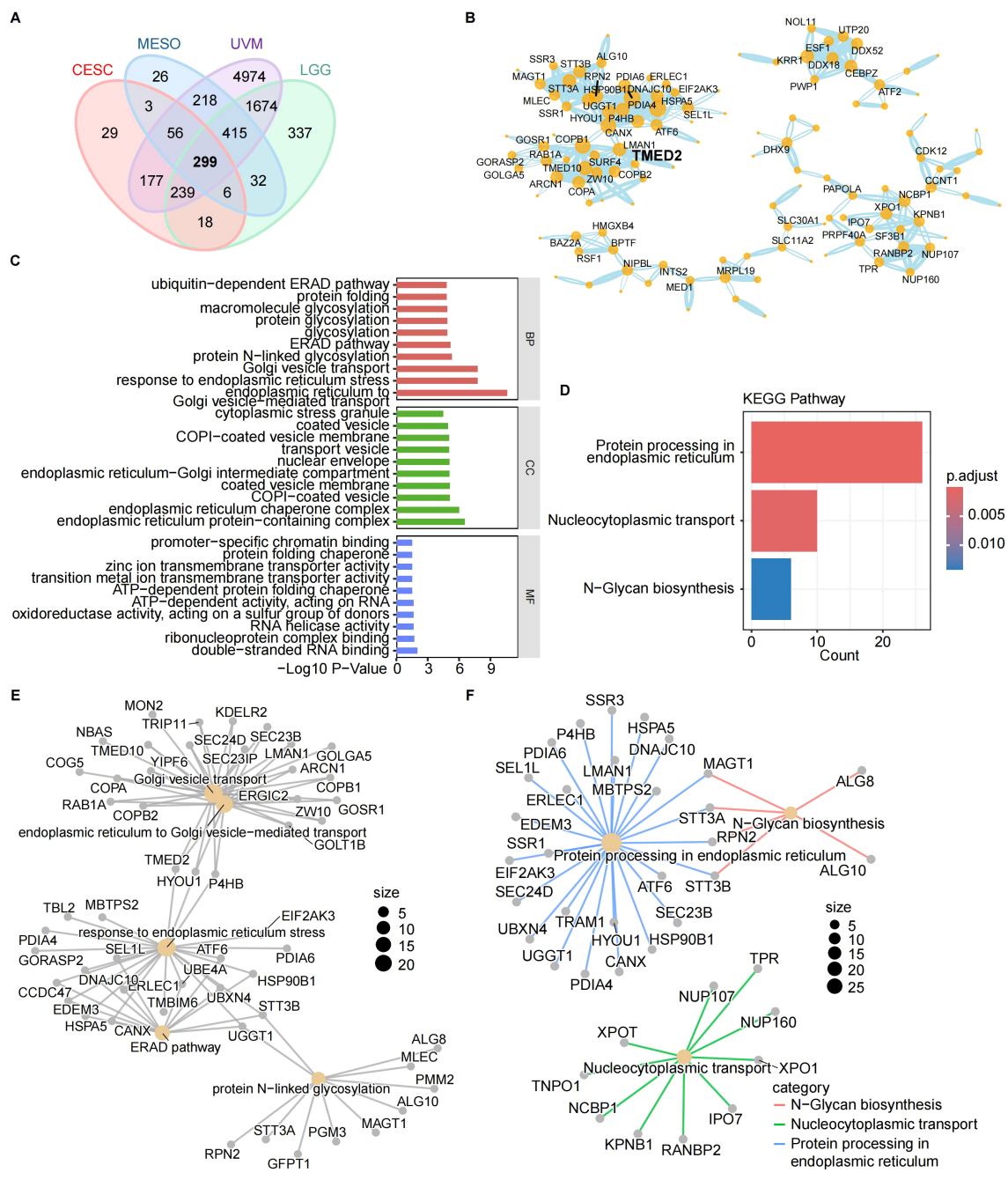


3.7 PPI network and enrichment pathways of TMED2 co-expressed genes

To explore whether TMED2 functions independently in cancer or collaborates with other genes for co-regulation, we attempted to construct its potential regulatory network. For this, we selected four cancer types that exhibited poor prognosis in the previous analysis, including CESC, MESO, LGG, and UVM, for in-depth investigation. Using Spearman correlation analysis, we identified genes that were co-expressed with TMED2, setting the criteria as a correlation

coefficient (R) > 0.5 and $P < 0.05$. We then performed a Venn diagram analysis to identify the intersection of these genes, ultimately selecting 299 genes co-expressed with TMED2 (Figure 6A). Subsequently, we utilized the STRING database to perform PPI network analysis on these 299 genes and TMED2 (Supplementary Figure S6), retaining the core nodes (Figure 6B). We then conducted GO and KEGG enrichment analyses for these genes (Figures 6D, F).

The results of the GO enrichment analysis revealed that multiple biological processes, cellular components, and molecular functions were significantly correlated with TMED2 expression.



Wang et al.,

FIGURE 6

The relationship between the expression of TMED2 and the expression of other genes. **(A)** Venn diagram of genes co-expressed with TMED2. **(B)** Core nodes of the PPI network of TMED2 and co-expressed genes. **(C-F)** Bar chart **(C)** and network diagram **(E)** for the Gene Ontology (GO) enrichment analysis of TMED2 and other genes; Bar chart **(D)** and network diagram **(F)** for the Kyoto Encyclopedia of Genes and Genomes (KEGG) enrichment analysis of TMED2 and other genes.

Notably, processes such as endoplasmic reticulum-associated degradation (ERAD), glycosylation modification, and endoplasmic reticulum stress were identified as key pathways (Figure 6C). In the enrichment network, TMED2 was found to be significantly associated with biological processes such as Golgi vesicle transport, transport from the endoplasmic reticulum to the

Golgi apparatus, ER stress, the ERAD pathway, and N-linked glycosylation (Figure 6E). KEGG Enrichment Analysis: The KEGG enrichment results showed a significant positive correlation between TMED2 expression and protein processing in the endoplasmic reticulum as well as nucleocytoplasmic transport (Figures 6D, F).

Notably, Golgi transport protein 1B (GOLT1B) was upregulated in most cancer tissues and was associated with immune cell infiltration, particularly the infiltration of T helper type 2 (Th2) cells (29). Additionally, the activation of transcription factor 6 (ATF6) following ER stress inhibits the expression of Δ Np63 α through the GRP78-AKT1-FOXO3a signaling pathway, thereby promoting breast cancer metastasis (30). Oligosaccharyltransferase subunit (STT3B) was shown to stabilize Epiregulin via N-glycosylation, which is crucial for PD-L1 upregulation and immune escape in head and neck squamous cell carcinoma (31).

These findings suggest that TMED2 does not act independently in cancer, but rather works synergistically with multiple genes within the same subcellular structures. It participates in various critical biological processes and signaling pathways, thereby influencing cancer development, progression, and immune evasion.

3.8 Drug sensitivity prediction of TMED2

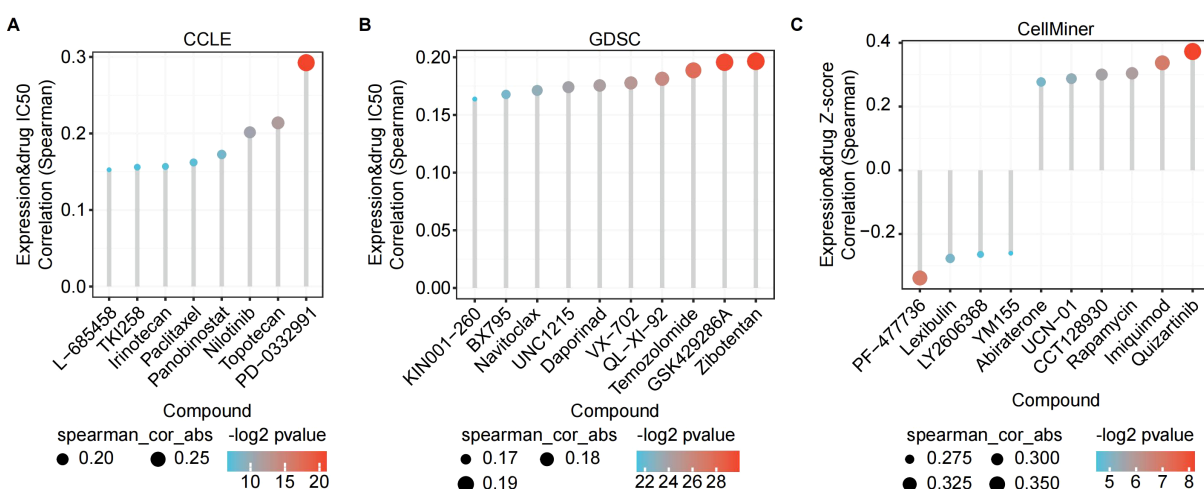
The above analysis indicates that TMED2 exhibits significant abnormal expression in various cancers and is closely associated with key biological processes such as tumor proliferation, differentiation, and immune evasion. These findings suggest that TMED2 could be a potential therapeutic target. Building on this, we further explored the correlation between small molecule drugs and TMED2 expression, aiming to provide more specific clues and directions for the development of drugs targeting TMED2. According to the CCLE dataset, Topotecan, Nilotinib, and PD-0332991 were the most three resistant drugs (Figure 7A). The top three resistant drugs associated with high TMED2 expression were Zibotentan, GSK429286A, and Temozolomide, according to the GDSC (Genomics of Drug Sensitivity in Cancer) dataset (Figure 7B). From the CellMiner dataset, the top four sensitive compounds were identified as Quizartinib, Imiquimod, Rapamycin, and CCT128930 (Figure 7C). These small molecules play antitumor roles in various cancers. Paclitaxel promotes tubulin polymerization into stable microtubules, inhibiting depolymerization and inducing mitotic arrest and apoptosis, making it a first-line treatment for breast cancer (32). Quizartinib, an FMS - like tyrosine kinase 3 (FLT3) inhibitor, specifically blocks FLT3 receptor tyrosine kinase activity, suppressing downstream signaling pathways and preventing FLT3-ITD-mutant acute myeloid leukemia cells from proliferating and surviving while inducing apoptosis (33). Our findings show that TMED2 expression is closely connected with drug treatment efficacy. The results of drug sensitivity analysis suggest that TMED2 may regulate these related pathways.

Rapamycin, and CCT128930 (Figure 7C). These small molecules play antitumor roles in various cancers. Paclitaxel promotes tubulin polymerization into stable microtubules, inhibiting depolymerization and inducing mitotic arrest and apoptosis, making it a first-line treatment for breast cancer (32). Quizartinib, an FMS - like tyrosine kinase 3 (FLT3) inhibitor, specifically blocks FLT3 receptor tyrosine kinase activity, suppressing downstream signaling pathways and preventing FLT3-ITD-mutant acute myeloid leukemia cells from proliferating and surviving while inducing apoptosis (33). Our findings show that TMED2 expression is closely connected with drug treatment efficacy. The results of drug sensitivity analysis suggest that TMED2 may regulate these related pathways.

3.9 TMED2 promotes glioma cell malignancy

According to our findings, TMED2 has high expression in malignancies. Results from single-cell sequencing further demonstrated that tumor cells might express more TMED2. Additionally, TMED2 expression has positive correlation with immunoregulatory pathways, like the cell cycle and PI3K/Akt signaling pathways, which influence tumor growth and expansion. These findings suggest that TMED2 might function as an oncogene in tumorigenesis and progression. We used U87 and U251 glioma cells with strong TMED2 expression in our *in vitro* experiments to confirm this hypothesis.

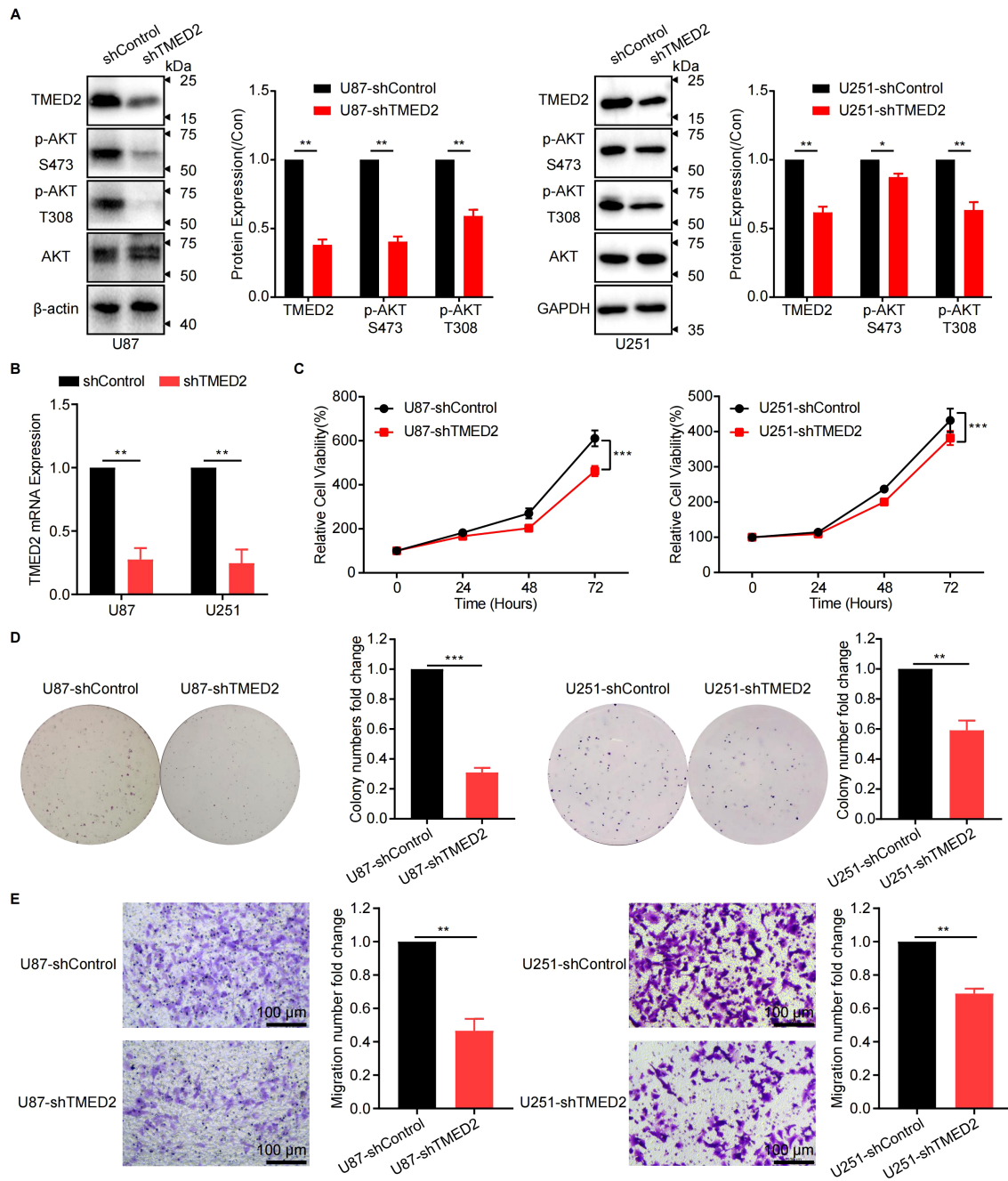
First, we knocked down TMED2 expression in U87 and U251 cells. The knockdown efficiency was assessed utilizing RT-qPCR and western blot (WB) analysis, which showed a substantial reduction in the levels of TMED2 mRNA and protein (Figures 8A, B). Phosphorylation of AKT was also downregulated, while total AKT protein levels remained unchanged compared to control cells (Figure 8A). This finding



Wang et al.,

FIGURE 7

The correlation between TMED2 expression and the small molecule drugs. The correlation between TMED2 expression and the small molecule drugs through CCLE (A), GDSC (B), and CellMiner (C) datasets.



Wang et al.,

FIGURE 8

Knockdown of TMED2 inhibited the proliferation and migration ability and AKT signaling pathway of glioma cells. **(A)** The expression of TMED2 and AKT signal in TMED2 knock-down cells was detected by WB in U251 and U87 cells (Data represent three independent experiments, using unpaired two-tailed Student's t-test). **(B)** The expression of TMED2 in TMED2 knock-down cells was detected by RT-qPCR in U251 and U87 cells. **(C)** The proliferation of U251 and U87 cells were evaluated by CCK8 assay (Data represent six independent experiments, using one-way ANOVA followed by Tukey's multiple comparisons tests). **(D)** The colony formation of U251 and U87 cells (Data represent three independent experiments, using unpaired two-tailed Student's t-test). **(E)** Cell migration of U251 and U87 cells was detected by the transwell assay (Data represent three independent experiments, using unpaired two-tailed Student's t-test). Scale bars = 100 µm. *P < 0.05, **P < 0.01, ***P < 0.001, ns, not significant.

indicates that TMED2 probably enhances the AKT signaling pathway, consistent with the GSEA enrichment results mentioned earlier.

Next, tumor phenotypes were assessed. CCK-8 assays demonstrated that TMED2 knockdown significantly suppressed

glioma cell proliferation (Figure 8C), a finding corroborated by reduced colony size in the plate colony formation assay (Figure 8D). These results suggest that TMED2 promotes glioma cell growth. Cell migration and invasion, critical factors in cancer metastasis and

recurrence, were evaluated using Transwell assays (Figure 8E). TMED2 knockdown greatly decreased the number of tumor cells migrating to the lower chamber, indicating that TMED2 enhances the migration and invasion capabilities of glioma cells.

4 Discussion

Research to date has showed that TMED2 plays a crucial role in cell division and proliferation, particularly in cancerous tumors (16–18). However, previous research has primarily concentrated on TMED2's function in specific cancer types, leaving its molecular characteristics in pan-cancer contexts underexplored. This study provides a comprehensive and in-depth investigation into the association between TMED2 expression and immunotherapy response in various cancers for the first time.

In our study, we employed a multidimensional approach leveraging extensive datasets. On the one hand, we examined TMED2 mRNA expression levels in cancer cell lines and tumor samples. Using TCGA and GTEx datasets, we observed a striking phenomenon: In comparison to normal samples, TMED2 expression was substantially elevated in almost all cancer cell lines. Single-cell sequencing further confirmed the high expression of TMED2 in tumor cells from cervical cancer, glioma, and mesothelioma. And its expression levels also varied across different cancer stages and tumor grade classifications. Additionally, analysis of the MuTarget dataset revealed disparities in the expression of TMED2 between mutant and wild-type (WT) groups in various cancers, shedding light on potential mutation mechanisms affecting TMED2 expression during tumorigenesis.

On the other hand, after clarifying the expression characteristics of TMED2 in cancer, we focused on exploring its potential as a therapeutic target for immune therapy in various solid cancers within the TIME. The results revealed clinically significant trends: patients with higher TMED2 expression levels derived less benefit from immunotherapies, including anti-PD-1/PD-L1 agents, nivolumab, pembrolizumab, and immune checkpoint inhibitors. To further explore the link between TMED2 and immunotherapy efficacy, we systematically evaluated the relationships between TMED2 and classical immune therapy biomarkers like MSI, TMB and TIDE scores. TMED2 was positively correlated with TMB in UCS, THYM, STAD, PAAD, LUAD, LGG, COAD, and BLCA but negatively correlated in THCA and CESC. TIDE scores, a validated predictive marker of immunotherapy response with high accuracy (34), were higher in patients with elevated TMED2 expression in most cancers, strongly suggesting that these patients may experience reduced immunotherapy efficacy.

The main goal of immunotherapy is to block immunological checkpoints. PD-1/PD-L1 and CTLA-4/B7 are two classical immune checkpoint pathways that adversely affect T-cell immunological activity, especially during critical periods of T-cell activation and proliferation (35–37). Our study examined the correlations between TMED2 and different immune checkpoints across tumors. TMED2 expression was positively connected with important immune checkpoint markers such as CD274, HAVCR2,

PDCD1LG2, and SIGLEC15 in numerous cancer types. However, we also observed that in certain cancers, such as CESC, LUAD, and THCA, many immune checkpoint molecules exhibited a negative correlation with TMED2 expression. This may suggest the complexity of different tissues, indicating that the expression of TMED2 is associated with the infiltration or activation of immune cells in various tissues.

In this study, we made two important discoveries. First, we utilized KEGG (Kyoto Encyclopedia of Genes and Genomes) analysis to investigate the role of TMED2 in tumors and explored its potential molecular mechanisms in cancer. We identified pathways like the cell cycle and PI3K/Akt signaling as being significantly associated with TMED2-mediated tumor immunity. This may be related to TMED2's role in protein transport (38–40). Furthermore, our previous studies reported that TMED2 enhances EGFR-AKT signaling in glioma by participating in EGFR recycling (41). These findings suggest that targeting TMED2 could suppress tumorigenesis by modulating these pathways.

Second, by constructing the potential regulatory network of TMED2, we revealed its synergistic action in various cancers. The results showed that TMED2, in collaboration with multiple genes, is involved in key biological processes such as endoplasmic reticulum-associated protein degradation, glycosylation modifications of proteins and other macromolecules, and endoplasmic reticulum stress. It is also significantly associated with signaling pathways like protein processing and nucleocytoplasmic transport. These findings suggest that TMED2 does not function independently in cancer but influences cancer initiation, progression, and immune evasion through its collaborative regulation with other genes. This discovery provides new insights into understanding the biological functions of TMED2 in cancer.

The above findings highlight the critical role of TMED2 as a potential therapeutic target, providing a theoretical foundation for drug development based on TMED2. With the rapid advancement of bioinformatics technologies, identifying optimal personalized treatment medications from common databases and computational modes has become a burgeoning trend in oncology research (42, 43). In this study, we discovered a range of small-molecule compounds that are linked to the expression of TMED2, which notably includes resistant compounds (Zilotentan, GSK429286A, Temozolomide, PD-0332991, Topotecan, Nilotinib) and sensitive compounds (Quizartinib, Imiquimod, Rapamycin, CCT128930). These findings provide potential directions for future TMED2-targeted drug development.

Our study deeply investigated TMED2's function in tumor immunology from a pan-cancer standpoint and verified that glioma cell proliferation and invasion are inhibited by TMED2 expression suppression. To confirm TMED2's function in cancer and clarify its mechanisms as a target for diagnosis and treatment, more *in vitro* and *in vivo* research is necessary.

5 Conclusion

In this study, we performed a preliminary yet systematic analysis of TMED2 with gene mutations, pathway enrichment,

classical immunotherapy biomarkers, drug treatment in pan-cancer. Our results demonstrate TMED2's enormous promise as a therapeutic target, its crucial role in immunity to tumors, and its potential as a prognostic biomarker for several cancer types.

Data availability statement

The datasets presented in this study can be found in online repositories. The names of the repository/repositories and accession number(s) can be found below: TCGA RNA-seq data and metadata were obtained from the UCSC Xena platform (<https://xenabrowser.net/>). The scRNA-seq data including cervical cancer (GSE168652), glioma (GSE131928) and mesothelioma (GSE201925) was downloaded from GEO (<https://www.ncbi.nlm.nih.gov/geo/>). The drug-susceptibility and cell line DATA was downloaded from GDSC (<https://www.cancerrxgene.org/>), CCLE (<https://sites.broadinstitute.org/ccle/>) and CellMiner (<https://discover.nci.nih.gov/cellminer/home.do>).

Ethics statement

Ethical approval was not required for the studies on humans in accordance with the local legislation and institutional requirements because only commercially available established cell lines were used.

Author contributions

ZW: Data curation, Formal Analysis, Investigation, Methodology, Software, Validation, Visualization, Writing – original draft, Writing – review & editing. CS: Conceptualization, Data curation, Formal Analysis, Investigation, Methodology, Project administration, Software, Supervision, Validation, Visualization, Writing – review & editing. PW: Data curation, Validation, Writing – review & editing. SL: Investigation, Validation, Writing – review & editing. XW: Conceptualization, Formal Analysis, Methodology, Project administration, Resources, Supervision, Validation, Writing – review & editing. YG: Conceptualization, Formal Analysis, Funding acquisition,

References

- Coulie PG, Van den Eynde BJ, van der Bruggen P, Boon T. Tumour antigens recognized by T lymphocytes: at the core of cancer immunotherapy. *Nat Rev Cancer*. (2014) 14:135–46. doi: 10.1038/nrc3670
- Marcus A, Gowen BG, Thompson TW, Iannello A, Ardolino M, Deng W, et al. Recognition of tumors by the innate immune system and natural killer cells. *Adv Immunol*. (2014) 122:91–128. doi: 10.1016/B978-0-12-800267-4.00003-1
- Porter DL, Levine BL, Kalos M, Bagg A, June CH. Chimeric antigen receptor-modified T cells in chronic lymphoid leukemia. *N Engl J Med*. (2011) 365:725–33. doi: 10.1056/NEJMoa1103849
- Topalian SL, Drake CG, Pardoll DM. Immune checkpoint blockade: a common denominator approach to cancer therapy. *Cancer Cell*. (2015) 27:450–61. doi: 10.1016/j.ccr.2015.03.001
- Jia Q, Wang A, Yuan Y, Zhu B, Long H. Heterogeneity of the tumor immune microenvironment and its clinical relevance. *Exp Hematol Oncol*. (2022) 11:24. doi: 10.1186/s40164-022-00277-y
- Chen Z, Elos MT, Viboolsittisiri SS, Gowan K, Leach SM, Rice M, et al. Combined deletion of Xrcc4 and Trp53 in mouse germinal center B cells leads to novel B cell lymphomas with clonal heterogeneity. *J Hematol Oncol*. (2016) 9:2. doi: 10.1186/s13045-015-0230-5
- Zhao-Wei R, Xue-Feng J, Gao-Tian X, Jin-Ling C, Jun LI, Shu-Ying LV. Study of the role of transmembrane emp24 domain-containing protein 2 in oral squamous cell carcinoma. *J Appl Sci*. (2025) 33:e20240305. doi: 10.1590/1678-7757-2024-0305
- Sial N, Saeed S, Ahmad M, Hameed Y, Rehman A, Abbas M, et al. Multi-omics analysis identified TMED2 as a shared potential biomarker in six subtypes of human cancer. *Int J Gen Med*. (2021) 14:7025–42. doi: 10.2147/IJGM.S327367

Investigation, Methodology, Project administration, Resources, Supervision, Validation, Writing – review & editing.

Funding

The author(s) declare that financial support was received for the research and/or publication of this article. This work is supported by Qingdao Marine Science and Technology Center (8–01 and No.2022NLM030003-4), National Natural Science Foundation of China (82273846), and Taishan Scholar Foundation of Shandong Province (No. tsqn202211058).

Conflict of interest

The authors declare that the research was conducted in the absence of any commercial or financial relationships that could be construed as a potential conflict of interest.

Generative AI statement

The author(s) declare that no Generative AI was used in the creation of this manuscript.

Publisher's note

All claims expressed in this article are solely those of the authors and do not necessarily represent those of their affiliated organizations, or those of the publisher, the editors and the reviewers. Any product that may be evaluated in this article, or claim that may be made by its manufacturer, is not guaranteed or endorsed by the publisher.

Supplementary material

The Supplementary Material for this article can be found online at: <https://www.frontiersin.org/articles/10.3389/fimmu.2025.1578627/full#supplementary-material>

9. Aber R, Chan W, Mugisha S, Jerome-Majewska LA. Transmembrane emp24 domain proteins in development and disease. *Genet Res (Camb)*. (2019) 101:e14. doi: 10.1017/S0016672319000090
10. Anwar MU, Sergeeva OA, Abrami L, Mesquita FS, Lukonin I, Amen T, et al. ER-Golgi-localized proteins TMED2 and TMED10 control the formation of plasma membrane lipid nanodomains. *Dev Cell*. (2022) 57:2334–46 e8. doi: 10.1016/j.devcel.2022.09.004
11. Nagae M, Hirata T, Morita-Matsumoto K, Theiler R, Fujita M, Kinoshita T, et al. 3D Structure and Interaction of p24beta and p24delta Golgi Dynamics Domains: Implication for p24 Complex Formation and Cargo Transport. *J Mol Biol*. (2016) 428:4087–99. doi: 10.1016/j.jmb.2016.08.023
12. Di Minin G, Holzner M, Grison A, Dumeau CE, Chan W, Monfort A, et al. TMED2 binding restricts SMO to the ER and Golgi compartments. *PLoS Biol*. (2022) 20:e3001596. doi: 10.1371/journal.pbio.3001596
13. Blum R, Pfeiffer F, Feick P, Nastainczyk W, Kohler B, Schäfer KH, et al. Intracellular localization and *in vivo* trafficking of p24A and p23. *J Cell Sci*. (1999) 112:537–48. doi: 10.1242/jcs.112.4.537
14. Bonifacino JS, Glick BS. The mechanisms of vesicle budding and fusion. *Cell*. (2004) 116:153–66. doi: 10.1016/S0092-8674(03)01079-1
15. Xiong X, Lu Y, Zhang L, Wang B, Zhao Y, Wang XJ, et al. Discovery of novel cell proliferation-enhancing gene by random siRNA library based combinatorial screening. *Comb Chem High Throughput Screen*. (2010) 13:798–806. doi: 10.2174/13862071079297240
16. Shi-Peng G, Chun-Lin C, Huan W, Fan-Liang M, Yong-Ning C, Ya-Di Z, et al. TMED2 promotes epithelial ovarian cancer growth. *Oncotarget*. (2017) 8:94151–65. doi: 10.18632/oncotarget.21593
17. Lin X, Liu J, Hu SF, Hu X. Increased expression of TMED2 is an unfavorable prognostic factor in patients with breast cancer. *Cancer Manag Res*. (2019) 11:2203–14. doi: 10.2147/CMAR.S192949
18. Gao W, Zhang ZW, Wang HY, Li XD, Peng WT, Guan HY, et al. TMED2/9/10 serve as biomarkers for poor prognosis in head and neck squamous carcinoma. *Front Genet*. (2022) 13:895281. doi: 10.3389/fgene.2022.895281
19. Fang Z, Song YX, Wo GQ, Zhou HL, Li L, Yang SY, et al. Screening of the novel immune-suppressive biomarkers of TMED family and whether knockdown of TMED2/3/4/9 inhibits cell migration and invasion in breast cancer. *Ann Transl Med*. (2022) 10:1280. doi: 10.21037/atm-22-5444
20. Zeng D, Fang Y, Qiu W, Luo P, Wang S, Shen R, et al. Enhancing immunotherapy investigations through multidimensional decoding of tumor microenvironment with IOBR 2.0. *Cell Rep Methods*. (2024) 4:100910. doi: 10.1016/j.crmeth.2024.100910
21. Yu G, Wang LG, Han Y, He QY. clusterProfiler: an R package for comparing biological themes among gene clusters. *Omics: A J Integr Biol*. (2012) 16:284–7. doi: 10.1089/omi.2011.0118
22. Mardinian K, Adashek JJ, Botta GP, Kato S, Kurzrock R. SMARCA4: implications of an altered chromatin-remodeling gene for cancer development and therapy. *Mol Cancer Ther*. (2021) 20:2341–51. doi: 10.1158/1535-7163.MCT-21-0433
23. Zhang Y, Sun C, Ma L, Xiao G, Gu Y, Yu W. O-GlcNAcylation promotes Malignancy and cisplatin resistance of lung cancer by stabilising NRF2. *Clin Transl Med*. (2024) 14:e70037. doi: 10.1002/ctm2.v14.10
24. Tang D, Kang R. NFE2L2 and ferroptosis resistance in cancer therapy. *Cancer Drug Resist*. (2024) 7:41. doi: 10.20517/cdr.2024.123
25. Fan M, Liu S, Zhang L, Gao S, Li R, Xiong X, et al. LGR6 acts as an oncogene and induces proliferation and migration of gastric cancer cells. *Crit Rev Eukaryot Gene Expr*. (2022) 32:11–20. doi: 10.1615/CritRevEukaryotGeneExpr.2021041271
26. Rui R, Zhou L, He S. Cancer immunotherapies: advances and bottlenecks. *Front Immunol*. (2023) 14:1212476. doi: 10.3389/fimmu.2023.1212476
27. Zhang Y, Zhang Z. The history and advances in cancer immunotherapy: understanding the characteristics of tumor-infiltrating immune cells and their therapeutic implications. *Cell Mol Immunol*. (2020) 17:807–21. doi: 10.1038/s41423-020-0488-6
28. Xi X, Wang Y, An G, Feng S, Zhu Q, Wu Z, et al. A novel shark VNAR antibody-based immunotoxin targeting TROP-2 for cancer therapy. *Acta Pharm Sin B*. (2024) 14:4806–18. doi: 10.1016/j.apsb.2024.08.023
29. Tian B, Pang Y, Gao Y, Meng Q, Xin L, Sun C, et al. A pan-cancer analysis of the oncogenic role of Golgi transport 1B in human tumors. *J Transl Int Med*. (2023) 11:433–48. doi: 10.2478/jtim-2023-0002
30. Wang H, Yang X, Deng L, Zhou X, Tao J, Wu Z, et al. ATF6 α inhibits Δ Np63 α expression to promote breast cancer metastasis by the GRP78-AKT1-FOXO3a signaling. *Cell Death Dis*. (2025) 16:289. doi: 10.1038/s41419-025-07619-8
31. Xu S, Wang H, Zhu Y, Han Y, Liu L, Zhang X, et al. Stabilization of EREG via STT3B-mediated N-glycosylation is critical for PDL1 upregulation and immune evasion in head and neck squamous cell carcinoma. *Int J Sci*. (2024) 16:47. doi: 10.1038/s41368-024-00311-1
32. Abu Samaan TM, Samec M, Liskova A, Kubatka P, Büselberg D. Paclitaxel's mechanistic and clinical effects on breast cancer. *Biomolecules*. (2019) 9:789. doi: 10.3390/biom9120789
33. Chao Q, Sprankle KG, Grotfeld RM, Lai AG, Carter TA, Velasco AM, et al. Identification of N-(5-tert-butyl-isoxazol-3-yl)-N'-[4-[7-(2-morpholin-4-yl-ethoxy)imidazo[2,1-b][1,3]benzothiazol-2-yl]phenyl]urea dihydrochloride (AC220), a uniquely potent, selective, and efficacious FMS-like tyrosine kinase-3 (FLT3) inhibitor. *J Med Chem*. (2009) 52:7808–16. doi: 10.1021/jm9007533
34. Jiang P, Gu S, Pan D, Fu J, Sahu A, Hu X, et al. Signatures of T cell dysfunction and exclusion predict cancer immunotherapy response. *Nat Med*. (2018) 24:1550–8. doi: 10.1038/s41591-018-0136-1
35. Zhang H, Dai Z, Wu W, Wang Z, Zhang N, Zhang L, et al. Regulatory mechanisms of immune checkpoints PD-L1 and CTLA-4 in cancer. *J Exp Clin Cancer Res*. (2021) 40:184. doi: 10.1186/s13046-021-01987-7
36. Tang Q, Chen Y, Li X, Long S, Shi Y, Yu Y, et al. The role of PD-1/PD-L1 and application of immune-checkpoint inhibitors in human cancers. *Front Immunol*. (2022) 13:964442. doi: 10.3389/fimmu.2022.964442
37. Li X, Wang Y, Wang Y, Xie H, Gong R, Wu X, et al. Anti-tumor activity of an α PD-L1-PE38 immunotoxin delivered by engineered Nissle 1917. *Int J Biol Macromol*. (2025) 295:139537. doi: 10.1016/j.ijbiomac.2025.139537
38. Buechling T, Chaudhary V, Spirohn K, Weiss M, Boutros M. p24 proteins are required for secretion of Wnt ligands. *EMBO Rep*. (2011) 12:1265–72. doi: 10.1038/embor.2011.212
39. Luo W, Wang Y, Reiser G. Proteinase-activated receptors, nucleotide P2Y receptors, and μ -opioid receptor-1B are under the control of the type I transmembrane proteins p23 and p24A in post-Golgi trafficking. *J Neurochem*. (2011) 117:71–81. doi: 10.1111/j.1471-4159.2011.07173.x
40. Fujita M, Watanabe R, Jaensch N, Romanova-Michaelides M, Satoh T, Kato M, et al. Sorting of GPI-anchored proteins into ER exit sites by p24 proteins is dependent on remodeled GPI. *J Cell Biol*. (2011) 194:61–75. doi: 10.1083/jcb.201012074
41. Sun C, Zhang Y, Wang Z, Chen J, Zhang J, Gu Y. TMED2 promotes glioma tumorigenesis by being involved in EGFR recycling transport. *Int J Biol Macromol*. (2024) 262:130055. doi: 10.1016/j.ijbiomac.2024.130055
42. Masoudi-Sobhanzadeh Y, Omidi Y, Amanlou M, Masoudi-Nejad A. Drug databases and their contributions to drug repurposing. *Genomics*. (2020) 112:1087–95. doi: 10.1016/j.ygeno.2019.06.021
43. Larson NB, Oberg AL, Adjei AA, Wang L. A clinician's guide to bioinformatics for next-generation sequencing. *J Thorac Oncol*. (2023) 18:143–57. doi: 10.1016/j.jtho.2022.11.006

Glossary

TCGA	The Cancer Genome Atlas	THCA	Thyroid carcinoma
CCLE	Cancer Cell Line Encyclopedia	THYM	Thymoma
GTEX	Genotype-Tissue Expression Program	UCEC	Uterine Corpus Endometrial Carcinoma
ACC	Adrenocortical carcinoma	UCS	Uterine Carcinosarcoma
BLCA	Bladder Urothelial Carcinoma	UVM	ocular melanomas
BRCA	Breast invasive carcinoma	OS	Overall survival
CESC	Cervical squamous cell carcinoma and endocervical adenocarcinoma	PFI	Progression Free Interval
CHOL	Cholangiocarcinoma	DSS	Disease-free survival
COAD	Colon adenocarcinoma	GO	Gene Ontology
DLBC	Lymphoid Neoplasm Diffuse Large B-cell Lymphoma	KEGG	Kyoto Encyclopedia of Genes and Genomes
ESCA	Esophageal carcinoma	GSEA	Gene set enrichment analysis
GBM	Glioblastoma multiforme	PPI	protein-protein interaction
HNSC	Head and Neck squamous cell carcinoma	PI3K	Phosphatidylinositol 3-kinase
KICH	Kidney Chromophobe	AKT	protein kinase B
KIRC	Kidney renal clear cell carcinoma	NOD-like receptor	Nucleotide-binding oligomerization domain-like receptors
KIRP	Kidney renal papillary cell carcinoma	TIDE	Tumor immune dysfunction and exclusion
LAML	Acute Myeloid Leukemia	ROC	Receiver Operating Characteristic
LGG	Brain Lower Grade Glioma	PD-1	Programmed cell death 1
LIHC	Liver hepatocellular carcinoma	PD-L1	Programmed cell death 1 ligand 1
LUAD	Lung adenocarcinoma	ERAD	endoplasmic reticulum-associated degradation
LUSC	Lung squamous cell carcinoma	GOLT1B	Golgi transport protein 1B
MESO	Mesothelioma	ATF6	the activation of transcription factor 6
OV	Ovarian serous cystadenocarcinoma	STT3B	Oligosaccharyltransferase subunit
PAAD	Pancreatic adenocarcinoma	ΔNp63α	Delta - N p63 alpha
PCPG	Pheochromocytoma and Paraganglioma	FOXO3a	Glucose - regulated Protein 78
PRAD	Prostate adenocarcinoma	GDSC	Oligosaccharyltransferase subunit
READ	Rectum adenocarcinoma	FLT3	Genomics of Drug Sensitivity in Cancer
SARC	Sarcoma	ITD	FMS - like tyrosine kinase 3
SKCM	Skin Cutaneous Melanoma	CTLA-4	Internal Tandem Duplication
STAD	Stomach adenocarcinoma		Cytotoxic T-lymphocyte-associated protein 4.
TGCT	Testicular Germ Cell Tumors		